

M-type channels selectively control bursting in rat dopaminergic neurons

Guillaume Drion^{1,2,*}, Maxime Bonjean^{3,*}, Olivier Waroux^{1,*}, Jacqueline Scuvée-Moreau¹, Jean-François Liégeois⁴, Terrence J. Sejnowski³, Rodolphe Sepulchre² and Vincent Seutin^{1°}

¹Laboratory of Pharmacology and GIGA Neurosciences, University of Liège, Belgium,

²Systems and Modeling, Department of Electricity, Electronics, and Computer science,

University of Liège, Belgium, ³Howard Hughes Medical Institute, The Salk Institute for

Biological Studies, and Department of Biological Sciences, the University of California, San

Diego, CA, USA, ⁴Laboratory of Medicinal Chemistry and Drug Research Center, University

of Liège, Belgium

* these three authors equally contributed to this work

°Corresponding author: Vincent Seutin, GIGA Neurosciences, Tour de Pathologie 2 (B36), C.H.U., B-4000 Sart Tilman/Liège 1, Belgium. (Tel: +32 43662525; Fax: +32 43662523)

V.Seutin@ulg.ac.be

Running title: M-channels and dopaminergic neurons

22 pages, 4 figures, 0 table, 9 equations

Total number of words: 6326 words; 182 words in the Abstract; 478 words in the Introduction

Supplementary material: 1 table and 6 figures

Keywords: M-current; substantia nigra; firing patterns; slow pacemakers; modeling; SK channels.

Summary

Midbrain dopaminergic neurons in the substantia nigra, pars compacta and ventral tegmental area are critically important in many physiological functions. These neurons exhibit firing patterns that include tonic slow pacemaking, irregular firing and bursting, and the amount of dopamine that is present in the synaptic cleft is much increased during bursting. The mechanisms responsible for the switch between these spiking patterns remain unclear. Using both *in vivo* recordings combined with microiontophoretic or intraperitoneal drug applications and *in vitro* experiments, we have found that M-type channels, which are present in midbrain dopaminergic cells, modulate the firing during bursting, without affecting the background low frequency pacemaker firing. Thus, a selective blocker of these channels, XE991, specifically potentiated burst firing. Computer modeling of the dopamine neuron confirmed the possibility of a differential influence of M-type channels on excitability during various firing patterns. Therefore, these channels may provide a novel target for the treatment of dopamine-related diseases, including Parkinson's disease and drug addiction. Moreover, our results demonstrate that the influence of M-type channels on the excitability of these slow pacemaker neurons is conditional upon their firing pattern.

Introduction

Midbrain dopaminergic (DA) neurons sustain important physiological functions such as control of motricity and signalling of positive error in reward prediction in the mesolimbic system (Schultz, 2007). A dysfunction of the DA system is implicated in the pathophysiology of Parkinson's disease, schizophrenia, and drug abuse (Iversen and Iversen, 2007). Under physiological conditions, DA neurons can switch between three distinct modes: tonic ("pacemaker"), irregular, and burst firing (Grace and Bunney, 1984; Brazhnik et al., 2008). Low frequency pacemaking of DA neurons mainly involves voltage-dependent Ca^{2+} channels (Puopolo et al., 2007). Because burst firing increases synaptic concentrations of dopamine (Chergui et al., 1994), many studies have focused on the factors controlling the switch to this firing pattern. It is generally agreed (see Overton and Clark, 1997) that bursting requires a glutamatergic input stimulating N-methyl-D-aspartate (NMDA) receptors. This has been further demonstrated recently by the observation that selective genetic inactivation of NMDA receptors in these neurons strongly disrupts burst firing, with many important behavioural consequences (Zweifel et al., 2009). On the other hand, activation of GABA_A receptors inhibits bursting because of their shunting effect on the oscillatory behavior (Tepper and Lee, 2007). Finally, both *in vitro* and *in vivo* experiments show that a reduction of a potassium conductance mediated by small conductance Ca^{2+} -activated K^+ (SK) channels greatly potentiates irregularity and/or bursting (Shepard and Bunney, 1988, 1991; Seutin et al., 1993; Nedergaard et al., 1993; Waroux et al., 2005; Ji and Shepard, 2006).

We and others recently described the presence of another K^+ current in DA neurons (Hansen et al., 2006; Koyama and Appel, 2006). This current had the typical electrophysiological signature (Brown and Adams, 1980; Kuffler and Sejnowski, 1983) and pharmacology of the M current, being enhanced by retigabine and blocked by 10,10-bis(4-pyridinylmethyl)-9(10*H*)-anthracenone dihydrochloride (XE991) (Tatulian et al., 2001; Wang

et al, 1998). Moreover, one of the subunits carrying M-currents (KCNQ4) was highly expressed in DA neurons (Hansen et al., 2006). However, blockade of the M-current by XE991 had only minor effects on the spontaneous firing of DA neurons in rat brain slices and *in vivo* (Hansen et al., 2006, and see Results). Thus, the M-current does not appear to act as a “brake” on low frequency firing. We hypothesized that, given its voltage-dependence, its rather slow activation rate and lack of inactivation, the M-current could be specifically involved in controlling the bursting behavior in these cells. Indeed, depolarized plateaus are observed in DA neurons during bursting (Grace and Bunney, 1984) and they are *a priori* sufficiently long-lasting (200-700 ms) to enable activation of M-channels. We tested this hypothesis using a combination of *in vivo* extracellular recordings of nigral DA neurons, intracellular recordings in a brain slice preparation, and computer modelling in which M-channels were added to a published model of DA neurons (Canavier and Landry, 2006).

Materials and methods

All procedures were carried out in accordance with guidelines of the European Communities Council Directive of 24 November 1986 (86/609/EEC) and were accepted by the Ethics Committee for Animal Use of the University of Liège (protocol 86).

In vivo experiments

Housing. Adult male Wistar rats were housed in groups of three or four, supplied with food and water *ad libitum*, and maintained on a 12 hours light/dark cycle.

Recordings. Rats (200-250 g) were anesthetized with chloral hydrate (400 mg/kg, i.p). Additional supplemental doses were injected intraperitoneally when necessary. Their temperature was maintained at 36 – 37 °C by means of a heating pad. The rats were placed in a stereotaxic apparatus (Model 902, Kopf). After removing a small part of the skull between

the lambda and the bregma, above the implantation point, the tip of the pipette was lowered into the brain at the following coordinates (with the lambda as reference) for the substantia nigra pars compacta (SN_C), 2 mm anterior, 1,8 – 2,2 mm lateral and 6 to 7 mm under the cortical surface, depending on the location in the frontal plane.

Electrodes and iontophoresis. All electrodes were made as described previously (Waroux et al., 2005) and consisted of a recording electrode and a five-barrel iontophoresis pipette glued together. For most experiments, each barrel was filled with one of the following solutions (dissolved in NaCl 30 mM): GABA (100 mM, pH 4); 30 mM NaCl (control solution in some experiments); *N*-methyl-laudoanine (NML) (10 mM, pH 7); SR 95531 (1-10 mM, pH 7) or XE991 (1 mM, pH 7); NaCl (0.5 M, current balancing); in some experiments, dopamine (100 mM, pH 7). The iontophoretic pipette was broken back at the tip to a diameter of approximately 20-30 μ m. The recording electrode had a tip diameter of 1-3 μ m and a resistance of 8-10 M Ω when filled with NaCl 0.9 %. A negative retention current of -10 nA was used between ejection periods. Drugs were ejected for 5 minutes, unless stated otherwise.

Action potential recordings and identification of neurons. Action potentials (amplitude: 200 to 1000 μ V) were passed through an impedance adapter and amplified one thousand times with a home made amplifier. They were displayed on an oscilloscope and fed to an analog digital interface (CED 1401) connected to a computer. Data were collected with the use of the “Spike 2” software (Cambridge Electronic Design, Cambridge, UK). Several scripts were used to analyse firing patterns and various characteristics of bursts.

Electrophysiological and pharmacological parameters were used in order to identify DA neurons as described (Waroux et al., 2005). *In vivo*, these neurons exhibit an irregular firing pattern with interspersed bursting episodes and long (> 2.5 ms), triphasic spikes (with a positive first phase), often displaying a prominent notch in the initial positive rising phase. They have a slow firing rate comprised between 0.5 and 5 Hz. In some experiments,

dopamine was iontophoresed as pharmacological control and always induced a slowing or complete cessation of the firing of the neurons, as expected.

Data analysis. To quantify the effect of SK channel blockers *in vivo*, we used established criteria of irregularity measurement of DA neuron firing *in vivo* (Grace and Bunney, 1984; Freeman et al., 1985). We quantified the number of spikes generated in bursts as a percentage of all spikes within a given period (1 minute). Parameters defining burst firing were at least three successive spikes with a maximal ISI of 80 ms between the two first spikes and a maximum of 160 ms for all intra-burst ISI's. Only experiments in which all data could be obtained were selected for further analysis, except for one i.p. experiment in which a very high % of spikes in bursts was observed during XE991 with 30 nA NML (97.21 %) before losing the cell and in which the same value was extrapolated for 60 and 90 nA. Experiments in which the firing rate differed by more than 25% between the first control period (before NML) and the end of the wash-out period of NML (before applying XE991) were also rejected.

Slice experiments

Methods were as described previously (Scuvée-Moreau et al., 2004). Briefly, male Wistar rats (150-200 g) were anaesthetized with chloral hydrate (400 mg/kg i.p.) and decapitated. The brain was rapidly removed and placed in cold (~ 4°C) artificial cerebro-spinal fluid of the following composition (in mM): NaCl 126, KCl 2.5, NaH₂PO₄ 1.2, MgCl₂ 1.2, CaCl₂ 2.4, glucose 11, NaHCO₃ 18, saturated with 95% O₂ and 5% CO₂ (pH 7.4). A block of tissue containing the midbrain was placed in a Vibratome (Lancer) filled with the same solution and cut in horizontal slices (thickness: 350 µm). The slice containing the SNc was completely immersed in a continuously flowing (~ 2 ml/min), heated solution (34 ± 0.5 °C) of the same

composition as indicated above. Intracellular recordings were made using glass microelectrodes filled with 2M KCl (resistance 70 to 150 M Ω). All recordings were made in the bridge balance mode, using an NPI BA-1S amplifier (NPI Electronic GmbH, Tamm, Germany). Membrane potentials and injected currents were recorded on a Gould TA240 chart recorder (Gould Instrument Systems, Valley View, OH) and on a Fluke Combiscope oscilloscope (Fluke Corp., Everett, WA). The Flukeview software was used for off-line analysis.

DA neurons had a slow (0.5-4 Hz) spontaneous firing rate, broad action potentials, a large I_h current and a prominent afterhyperpolarization (Scuvée-Moreau *et al.*, 2002).

Statistics. Because a Shapiro-Wilk test showed that some *in vivo* data were not normally distributed, these experiments were analyzed with a non-parametric test (Wilcoxon test for paired values). The slice experiments were analyzed with a repeated measures ANOVA test, followed by a post-hoc Newman Keuls test. Simulation data were analyzed using Student's *t* tests for paired values. The level of significance was set at $P < 0.05$ in all cases. All statistical analyses were run on Statistica^o (version 8) (StatSoft, Tulsa, OK, USA). For clarity, all the results are expressed as means \pm SEM.

Drugs.

Sources of drugs used were as follows: apamin, dopamine and GABA were obtained from Sigma (St Louis, MO). NML was synthesized and evaluated in our laboratory (Scuvée-Moreau *et al.*, 2002). XE991, CGP55845, CNQX, and APV were purchased from Tocris Cookson (Bristol, UK). The GABA_A antagonist 2-(3-carboxypropyl)-3-amino-6-(4-methoxyphenyl) pyridazinium bromide (SR95531) was a gift from Sanofi (Paris, France).

Computational Methods

The computational model of a single DA neuron was based on Canavier and Landry (2006) with some modifications (Bonjean et al., 2007). The model included a soma, four branched proximal, and eight distal dendrites.

All compartments were capable of generating action potentials and contained a fast sodium current I_{Na} , a delayed rectifier potassium current $I_{K,dr}$, a transient outward potassium current $I_{K,A}$, a leak current I_{leak} , and a Na^+/K^+ pump, as well as sodium dynamics and a sodium balance ruled by the following equations:

$$\begin{aligned}\frac{d[Na^+]_{in,s}}{dt} &= \frac{4f_s(-I_{Na,s} - I_{Leak,Na,s} - 3I_{Na,pump,s})}{d_s F} \\ \frac{d[Na^+]_{in,p}}{dt} &= \frac{4f_p(-I_{Na,p} - I_{Leak,Na,p} - I_{SYN,Na,p} - 3I_{Na,pump,p})}{d_p F} \\ \frac{d[Na^+]_{in,d}}{dt} &= \frac{4f_d(-I_{Na,d} - I_{Leak,Na,d} - I_{SYN,Na,d} - 3I_{Na,pump,d})}{d_d F}\end{aligned}$$

where F is the Faraday constant, the subscripts s , p , and d denote the compartment (soma, proximal, and distal), and I_{Syn} is the sum of synaptic currents mediated by Na^+ , i.e.

$$\begin{aligned}I_{syn,Na,p} &= I_{NMDA,Na,p} + I_{AMPA,Na,p} \\ I_{syn,Na,d} &= I_{NMDA,Na,d} + I_{AMPA,Na,d}\end{aligned}$$

The soma contained a hyperpolarization-activated cation current I_H , and an SK K^+ -current activated by calcium. Calcium entered the soma through voltage-activated T-type, N-type and L-type currents and calcium was removed with a calcium pump. M-type channels, producing the $I_{K,M}$ current (M-current), were also included in the somatic compartment (Bonjean et al., 2007), with the following dynamics :

$$\begin{aligned}I_{K,M} &= g_{K,M} n(V - E_K), \\ \frac{dn}{dt} &= \alpha_n(1 - n) - \beta_n n,\end{aligned}$$

where the channel opening and closing rate constants α_n and β_n are defined by (Bibbig et al., 2001):

$$\alpha_n = \frac{0.02}{1 + \exp\left[\frac{-V - 20}{5}\right]},$$
$$\beta_n = 0.01 \exp\left[\frac{-V - 43}{18}\right]$$

The maximal conductance of the M-current was set to 300 $\mu\text{S}/\text{cm}^2$, giving a conductance of 196 $\mu\text{S}/\text{cm}^2$ at -45 mV. This is ~ 5 times the conductance that can be calculated from published data (36 $\mu\text{S}/\text{cm}^2$: Koyama and Appel, 2006), which were obtained using dissociated DA neurons. When we used the value of the conductance found experimentally, the effect was qualitatively similar, but much less robust (see Results). Possible reasons for this discrepancy include an underestimation of the conductance in the experiments because of damage to the channels produced by the dissociation procedure or because of a higher current density in the dendrites versus the soma. Alternatively, some fine adjustments of the model may be needed. Indeed, many of the parameters that have been implemented in the model have not been

directly measured in DA neurons, but have usually been taken from published data on other types of neurons. Moreover, other features of DA neurons (presumably high density of Na_v channels in the axonal initial segment, axon originating from a primary dendrite in many DA neurons) have not been taken into account. The development of a completely accurate model will therefore only be possible when all this information is available.

Synaptic AMPA and NMDA receptors, mediating I_{AMPA} and I_{NMDA} currents, were located on the dendritic compartments. GABA_A receptors, mediating $I_{\text{GABA,A}}$ current, were located both on somatic and dendritic compartments with a density ratio of 1:10.

All currents followed a Hodgkin-Huxley kinetic scheme (Hodgkin and Huxley, 1952). The dynamics of the synaptic currents were modeled with a two-state kinetic scheme (Destexhe et al., 1994). Glutamatergic synaptic events were generated by a Poisson stochastic process, which mimicked *in-vivo* like activity (Canavier and Landry, 2006).

Simulations were performed under the NEURON modeling program, with a Runge-Kutta 4th order integration method, on a Pentium 4 3 GHz. Analyses of computational data were carried out with MATLAB 7 (R14).

The mean charge transfer through M-channels in each condition was calculated by taking the mean values of the simulated M-current in the model for 6 simulations. The M-current density before action potentials was obtained by measuring the instantaneous values of the M-current 20 ms before the onset of action potentials (which was defined as the crossing of -40mV

during its ascending phase). These values were obtained before 260 events in control conditions and 350 events during $I_{K,SK}$ inhibition.

In a few simulations (Fig. 3d), the cytoplasmic calcium concentration $[Ca^{2+}]_{in}$ in the model was varied and the firing frequency of the simulated trace was computed for each of these values. The intra-burst firing frequency was subsequently plotted as a function of the calcium concentration. These particular simulations were performed in the absence of synaptic afferents and while $[Na^+]_{in}$ was fixed at 3.8, 2.8 and 4 mM for the soma, the proximal dendrites and the distal dendrites, respectively.

Results

Effect of systemic and local application of XE991 on the firing of DA neurons

In a first series of experiments, we studied the impact of intraperitoneally administered XE991 (3 mg/kg i.p.) on the firing of DA neurons. In previous *in vitro* experiments, we had demonstrated that this compound is a specific blocker of the M current in these cells: thus, it had no effect on the shape of action potentials, on the resting membrane potential or on the medium-duration afterhyperpolarization induced by the opening of SK channels (Hansen et al., 2006).

The effect of i.p. XE991 was variable, ranging from no change to a large inhibitory effect ($n = 6$) (Supplementary Figure 1). This could be due to a mixture of direct and indirect factors, since KCNQ channels are also expressed by many neurons that project to DA neurons. The firing of rat DA neurons is under the inhibitory control of GABA_A receptors (Tepper and Lee, 2007). The experiments were therefore repeated while iontophoresing a pharmacologically active (Supplementary Table 1) amount of the specific GABA_A antagonist SR95531. Under these conditions, XE991 had no effect on the spontaneous firing rate or pattern (Figure 1a) of DA neurons: firing rates were 2.9 ± 0.4 and 3.1 ± 0.4 spikes/s (mean \pm SEM) ($P = 0.25$,

Wilcoxon test, $n = 6$) in control conditions and in the presence of XE991, respectively. The percentage of spikes in bursts (see Methods) was 4.2 ± 2.3 and 3.7 ± 1.0 %, respectively ($P = 0.89$, Wilcoxon test, $n = 6$).

To evaluate the ability of the neurons to fire in bursts, we iontophored a reversibly acting blocker of small conductance Ca^{2+} -activated K^+ (SK) channels, *N*-methyl-laudanosine (NML, 10 mM) (Scuvée-Moreau et al., 2002). This procedure facilitates bursting in these cells in an intensity-dependent manner (Waroux et al., 2005); that is, the percentage of spikes fired in bursts increases as a function of current intensity (30, 60 or 90 nA).

In order to assess the physiological relevance of our model of bursting, we compared the characteristics of natural (i.e. spontaneous) and NML-induced bursts in the absence of any other pharmacological agent. They were found to be remarkably similar (Supplementary figures 2 and 3; see also Waroux et al., 2005). Thus, the mean value of the interspike intervals (ISI's) was similar in both cases, as was the fact that the first ISI was shorter than the next ones, the values of which were close to 100 ms. Burst size histograms showed that the relative frequency of the bursts as a function of their number of spikes was similar in both conditions (Supplementary Fig. 3a). Importantly, a progressive decrease in the amplitude of the extracellularly recorded action potentials was observed in both natural and NML-induced bursts, and this decrease had a mean amplitude (~ 20 %, Supplementary Fig. 3b) that was similar in both conditions. The latter data strongly suggest that the membrane potential changes underlying both types of bursts are quantitatively similar, confirming the validity of our model. Moreover, all these parameters were similar to those described previously (e.g. Grace and Bunney, 1984).

We next examined the influence of XE991 on NML-induced bursts. Figure 1a shows that i.p. administered XE991 potentiated NML-induced bursting when GABA_A receptors of DA neurons were blocked with SR95531. The amplitude of the effect of the M-channel blocker

was dependent on the NML iontophoresis current intensity. Thus, during 30 nA NML, XE991 increased the percentage of spikes in bursts from 16 ± 8 to 39 ± 15 % ($P = 0.028$, Wilcoxon test, $n = 6$). A similar effect was seen during 60 nA (from 29 ± 13 to 50 ± 13 %, $P = 0.028$, Wilcoxon test). At 90 nA, no significant effect was observed (from 41 ± 14 to 54 ± 12 %, $P = 0.17$, Wilcoxon test), probably because of a saturation effect. Control i.p. injections of the vehicle had no discernible effect ($n = 3$, Supplementary Fig. 4a).

In order to test whether XE991 acts directly on DA neurons, we next iontophored it onto the recorded neurons. For these experiments, we chose not to use a GABA_A antagonist in order to mimick as closely as possible the physiological situation. Moreover, local application of XE991 made any indirect effect of the drug unlikely. As shown in figure 1b, the effects of the drug were quite similar to those observed after i.p. injection. Thus, XE991 (100 nA) had no effect on tonic firing (3.4 ± 0.6 and 3.5 ± 0.6 spikes/s in control conditions and in the presence of XE991, respectively, $P = 0.21$, Wilcoxon test, $n = 8$), but increased the percentage of spikes in bursts from 10 ± 8 to 26 ± 9 % during 30 nA NML ($P = 0.018$, Wilcoxon test) and from 37 ± 10 to 53 ± 11 % during 60 nA ($P = 0.018$, Wilcoxon test). At 90 nA, the increase (46 ± 12 to 59 ± 9 %) was also significant ($P = 0.049$, Wilcoxon test) (Fig. 1c, lower panel). Iontophoresis of the vehicle had no effect at any intensity of NML iontophoresis ($n = 5$, Supplementary Fig. 4b).

A close inspection of the bursting behaviour revealed that the M-channel blocker also modified it qualitatively. For example, figure 1d shows that, when administered either i.p. or by iontophoresis, it increased the proportion of short ISI's during 60 nA (other results are shown in Supplementary Fig. 5). This is also apparent in the insets of figure 1a and b.

XE991 facilitates fast firing induced by current injection in vitro

In order to confirm the ability of XE to facilitate the occurrence of short interspike intervals in DA neurons, we performed intracellular recordings of these neurons in slices containing the SNc. This recording mode was chosen because it is the least likely to disrupt intracellular pathways, which are critical in the control of M-channels (Delmas and Brown, 2005). For these experiments, we superfused the slices with blockers of synaptic transmission (10 μ M CNQX, 50 μ M APV, 10 μ M SR95531 and 1 μ M CGP55845) in order to exclude indirect effects. A supramaximal concentration of the SK blocker apamin (300 nM) was used to mimic our *in vivo* conditions. Neurons were hyperpolarized to -60 mV by negative current injection (-50 to -150 pA) and depolarizing pulses (50-150 pA, 800 ms) were given repeatedly to evoke spikes. In these conditions, 10 μ M XE991 significantly increased the number of spikes from 3.2 ± 0.5 to 5.2 ± 0.9 after 10 minutes (Fig. 2) ($n = 4$) ($F = 17.1$, $P = 0.000$, repeated measures ANOVA; values after the 5th minute of XE application were significantly different from those of the control condition (Newman-Keuls test); see figure 2 for the various levels of significance). On the other hand, it had no effect on the baseline voltage. XE991 had no significant effect in the absence of apamin (not shown, data from Hansen et al., 2006).

Computer modelling of the effect of the M-current

We next explored the mechanism underlying our *in vivo* observations in a model of a DA neuron (Canavier and Landry, 2006), which included amongst others a SK current and a M-current (see Methods). The activation of synaptic currents was modeled by a Poisson process. Many of the electrophysiological features observed in DA neurons, including low frequency pacemaker activity and burst firing were reproduced in the model, which confirmed that the absence of M-current potentiates SK blockade-induced bursting (Fig. 3a). Quantitative analysis of 6 different model neurons (using different synaptic input patterns) reproduced the experimental results (Fig 3b, Supplementary Fig. 5d). This effect was robust when the M-

conductance was 5 times that measured experimentally (Koyama and Appel, 2006, see Methods). When the conductance value was identical to the measured one, the effect was very modest (Supplementary Fig. 6).

The model also confirmed the ability of M-current blockade to increase the proportion of short ISI's within bursts (Fig. 3c). A plot of intra-burst firing frequency versus $[Ca^{2+}]_{in}$ (Fig. 3d) shows the predicted effect of the SK and M conductances on the firing behavior of the model neuron. As compared to the control condition, SK blockade allowed faster firing at intermediate $[Ca^{2+}]_{in}$ values. Additional block of M channels shifted the curve to even higher frequencies (as observed experimentally by a higher proportion of short ISI's).

We next analyzed the M-current quantitatively in the model, both when the SK conductance was maximal and when it was set to 0. The charge transfer through the M conductance was higher in the second condition (Fig. 4a,b). The difference was even more striking when considering the mean charge transfer at 20 ms before the onset of action potentials in both conditions (Fig. 4c, see Methods). Clearly, the M-current completely deactivates between two successive action potentials during low frequency pacemaker or irregular firing, but not when the membrane potential is more depolarized during SK blockade (Fig. 4a).

Discussion

Taken together, the experimental and modeling data demonstrate that the M-current selectively gates the bursting behavior in DA neurons. The effect that we observe experimentally *in vivo* is most probably due to the blockade of somato-dendritic M channels, whose existence has been demonstrated experimentally (see Introduction). Indeed, the burst enhancing effect is observed when GABA_A receptors (the major substrate of afferent inhibition in the rat: Tepper and Lee, 2006) are blocked. Furthermore, our slice experiments confirm that XE991 facilitates fast firing in these neurons by a direct effect. Although the

precise mechanism(s) underlying natural bursts in DA neurons *in vivo* is (are) not known, our demonstration that natural and NML-induced bursts have similar characteristics allows to generalize our findings to the physiological situation.

Our results show that low frequency pacemaker firing is largely unaffected by XE991, presumably because the membrane potential does not reach sufficiently depolarized levels for long enough for M-channels to become substantially activated (Fig. 4a). The M-channels activate during each action potential during this firing pattern, but quickly deactivate, so that no current is flowing through them at the onset of the next spike. On the contrary, during burst firing, complete deactivation is prevented by fast firing during depolarized plateaus and this allows the channels to exert their inhibitory effect under these circumstances.

Besides its quantitative enhancement of burst firing, suppression of the M-current also alters the quality of the bursts, with a relative enrichment of very short ISIs. This effect is likely to be biologically important because it will increase the saturation of dopamine transporters at the terminals and hence sharpen the increases in the concentration of dopamine. The effect of M-current blockade on the distribution of ISI's was more spectacular in the model than in the experiments (compare Supplementary Fig 5 b and d). This is probably due to the fact that the dominant repolarizing currents (other than the SK current) after the action potential deactivate too quickly in the model. This leads to a high proportion of closely spaced action potentials.

Our results on XE991 differ from those of Sotty et al. (2009), who observed a significant increase in bursting in the same species when the M-current blocker was administered alone (i.e. without SK blockade). There are several possible reasons for this discrepancy: 1) their recordings were made in the ventral tegmental area and it cannot be excluded that the density and/or topography of M channels is different in the two areas. Moreover, the tone of excitatory and/or inhibitory afferents may also be different. This may in turn induce

differences in the amount of bursting in control conditions. 2) XE991 was administered i.v. (versus i.p. in our case) and the effect was observed at 1 and 2 mg/kg. It is probable that brain concentrations achieved in their experiments were higher than in our i.p. experiments. However, we also did not see an effect of XE991 alone in our iontophoresis experiments, even when using a higher concentration of XE991 (10 mM instead of 1 mM, not shown). 3) the data analysis is different in the two studies. Sotty et al. analyzed the “percent changes in burst firing”, whereas we used a more conservative analysis, using the absolute value of the proportion of spikes that occur in bursts. We felt that the latter analysis is preferable because the first one may give too much importance to changes occurring in neurons with a small percentage of spikes in bursts (a change from 1 to 5% will be counted as a 500% change, whereas a change from 30 to 60% will be considered 200%). On the other hand, their conclusions on the influence of retigabine on DA neurons are globally similar to ours (Hansen et al., 2006).

Our results demonstrate a novel pathway for selectively altering the transient responses of DA neurons to excitatory inputs without changing their low frequency tonic activity. Given the variety of intracellular pathways that control M-current in CNS neurons (Delmas and Brown, 2005), it may offer a powerful means by which various afferent neurotransmitters can fine tune DA transmission. One obvious candidate is acetylcholine, which blocks the M-current via M1/M3 receptors in many types of neurons. There is ample evidence for an excitatory and burst-enhancing effect of muscarinic agonists on midbrain DA neurons (Gronier and Rasmussen, 1998; Miller and Blaha, 2005). However, acetylcholine obviously has multiple effects – including inhibitory ones - on DA neuron excitability, depending on the concentration of synaptic acetylcholine and its duration of action (Fiorillo and Williams, 2000). Pharmacological modulation of the M-current should have a major impact on DA

signalling that could be exploited therapeutically in the future (see Sotty et al., 2009 for further discussion).

More generally, our results demonstrate that M-channels do not reduce spontaneous low frequency firing in DA neurons. This is because of the parameters of their activation and deactivation relative to the voltage trajectory during pacemaking. However, their presence makes these neurons relatively insensitive to excitatory inputs. Therefore, modulation of this conductance may selectively control the excitability of these neurons when they are in bursting mode. This may be an advantage in some behavioural contexts.

Acknowledgments

Supported by grant n° 9.4560.03 from the F.R.S-FNRS (VS, J-FL), by a grant from the Belgian Science Policy (IAP 6/31) (VS), and by grants from the Howard Hugues Medical Institute (TJS), BAEF-Fulbright (MB) and NSF-NIH (CRCNS) (TJS & MB).

J.-F. L. is Research Director of the F.R.S-FNRS. We thank Dr. Laurence Seidel and Mrs. Livia Alleva (University of Liège) for her help with the statistical analysis and Drs. Margarita Behrens and Jay Coggan (Salk Institute) for helpful discussions. We also thank Dr. Bruce P. Bean (Harvard University) for reading an earlier version of the manuscript.

References

Bibbig, A., Faulkner, H.J., Whittington, M.A. & Traub, R.D. (2001) Self-organized synaptic plasticity contributes to the shaping of γ and β oscillations *in vitro*. *J. Neurosci.*, **21**, 9053-9067.

Bonjean, M., Waroux, O., Engel, D., Dang-Vu, T., Phillips, C., Lamy, C., Scuvée-Moreau, J., Sepulchre, R., Maquet, P. & Seutin V (2007) Effect of the M-current on the excitability of midbrain dopaminergic neurons: a computational study. *Soc. Neurosci. Abstr.*, **681.6**.

Brazhnik, E., Shah, F. & Tepper, J.M. (2008) GABAergic afferents activate both GABA_A and GABA_B receptors in mouse substantia nigra dopaminergic neurons in vivo. *J. Neurosci.*, **28**, 10386-10398.

Brown, D.A. & Adams, P.R. (1980) Muscarinic suppression of a novel voltage-sensitive K⁺ current in a vertebrate neurone. *Nature*, **283**, 673-676.

Canavier, C.C. & Landry, R.S. (2006) An increase in AMPA and a decrease in SK conductance increase burst firing by different mechanisms in a model of a dopamine neuron in vivo. *J. Neurophysiol.*, **96**, 2549-2563.

Chergui, K., Suaud-Chagny, M.M. & Gonon, F. (1994) Nonlinear relationship between impulse flow, dopamine release and dopamine elimination in the rat brain in vivo. *Neuroscience*, **62**, 641-645.

Delmas, P. & Brown, D.A. (2005) Pathways modulating neural KCNQ/M (Kv7) potassium channels. *Nat. Rev. Neurosci.*, **6**, 850-862.

Destexhe, A., Mainen, Z.F. & Sejnowski, T.J. (1994) Synthesis of models for excitable membranes, synaptic transmission and neuromodulation using a common kinetic formalism. *J. Comput. Neurosci.*, **1**, 195-230.

Fiorillo, C.D. & Williams, J.T. (2000) Cholinergic inhibition of ventral midbrain dopamine neurons. *J. Neurosci.*, **20**, 7855-7860.

Freeman, A.S., Meltzer, L.T. & Bunney, B.S. (1985) Firing properties of substantia nigra dopaminergic neurons in freely moving rats. *Life Sci.*, **36**, 1983-1994.

Grace, A.A. & Bunney, B.S. (1984) The control of firing pattern in nigral dopamine neurons: burst firing. *J. Neurosci.*, **4**, 2877-2890.

- Gronier, B. & Rasmussen K. (1998) Activation of midbrain presumed dopaminergic neurones by muscarinic cholinergic receptors: an in vivo electrophysiological study. *Br. J. Pharmacol.*, **124**, 455-464.
- Hansen, H.H., Ebbesen, C., Mathiesen, C., Weikop, P., Ronn, L.C., Waroux, O., Scuvée-Moreau, J., Seutin, V. & Mikkelsen, J.D. (2006) The KCNQ channel opener retigabine inhibits the activity of mesencephalic dopaminergic systems of the rat. *J. Pharmacol. Exp. Ther.*, **318**, 1006-1019.
- Hodgkin, A.L. & Huxley, A.F. (1952) A quantitative description of membrane current and its application to conduction and excitation in nerve. *J. Physiol.*, **117**, 500-544.
- Iversen, S.D. & Iversen, L.L. (2007) Dopamine : 50 years in perspective. *Trends Neurosci.*, **30**, 188-193.
- Ji, H. & Shepard, P.D. (2006) SK Ca²⁺-activated K⁺ channel ligands alter the firing pattern of dopamine-containing neurons in vivo. *Neuroscience*, **140**, 623-633.
- Koyama, S. & Appel, S.B. (2006) Characterization of M-current in ventral tegmental area dopamine neurons. *J. Neurophysiol.*, **96**, 535-543.
- Kuffler, S.W. & Sejnowski, T.J. (1983) Peptidergic and muscarinic excitation at amphibian sympathetic synapses. *J. Physiol.*, **341**, 257-278.
- Miller, A.D. & Blaha, C.D. (2005) Midbrain muscarinic receptor mechanisms underlying regulation of mesoaccumbens and nigrostriatal dopaminergic transmission in the rat. *Eur. J. Neurosci.*, **21**, 1837-1846.
- Nedergaard, S., Flatman, J.A. & Engberg, I. (1993) Nifedipine- and omega-conotoxin-sensitive Ca²⁺ conductances in guinea-pig substantia nigra pars compacta neurones. *J. Physiol.*, **466**, 727-747.
- Overton, P.G. & Clark, D. (1997) Burst firing in midbrain dopaminergic neurons. *Brain Res. Rev.*, **25**, 312-334.

Puopolo, M., Raviola, E. & Bean, B.P. (2007) Roles of subthreshold calcium current and sodium current in spontaneous firing of mouse midbrain dopamine neurons. *J. Neurosci.*, **27**, 645-656.

Schultz, W. (2007) Behavioral dopamine signals. *Trends Neurosci.*, **30**, 203-210.

Scuvée-Moreau, J., Liégeois, J.-F., Massotte, L. & Seutin, V. (2002) Methyl-laundanosine: a new pharmacological tool to investigate the function of small conductance Ca²⁺-activated K⁺ (SK) channels. *J. Pharmacol. Exp. Ther.*, **302**, 1176-1183.

Scuvée-Moreau, J., Boland, A., Graulich, A., Van Overmeire, L., D'hoedt, D., Graulich-Lorge, F., Thomas, E., Abras, A., Stocker, M., Liégeois, J.-F. & Seutin, V. (2004) Electrophysiological characterization of the SK channel blockers methyl-laundanosine and methyl-noscapine in cell lines and rat brain slices. *Br. J. Pharmacol.*, **143**, 753-764.

Seutin, V., Johnson, S.W. & North, R.A. (1993) Apamin increases NMDA-induced burst firing of rat mesencephalic dopamine neurons. *Brain Res.*, **630**, 341-344.

Shepard, P.D. & Bunney, B.S. (1988) Effect of apamin on the discharge properties of putative dopamine-containing neurons in vitro. *Brain Res.*, **463**, 380-384.

Shepard, P.D. & Bunney, B.S. (1991) Repetitive firing properties of putative dopamine-containing neurons in vitro: regulation by an apamin-sensitive Ca²⁺-activated K⁺ conductance. *Exp. Brain Res.*, **86**, 141-150.

Sotty, F., Damgaard, T., Montezinho, L.P., Mork, A., Olsen, C.K., Bundgaard, C. & Husum, H. (2009) Antipsychotic-like effect of retigabine [N-(2-Amino-4-(fluorobenzylamino)-phenyl)carbamic acid ester], a KCNQ potassium channel opener, via modulation of mesolimbic dopaminergic neurotransmission. *J. Pharmacol. Exp. Ther.*, **328**, 951-962.

Tatulian, L., Delmas, P., Abogadie, F.C. & Brown, D.A. (2001) Activation of expressed KCNQ potassium currents and native neuronal M-type potassium currents by the anti-convulsant drug retigabine. *J. Neurosci.*, **21**, 5535-5545.

Tepper, J.M. & Lee, C.R. (2007) GABAergic control of substantia nigra dopaminergic neurons. *Prog. Brain Res.*, **160**: 189-208.

Wang, H.S., Pan, Z., Shi, W., Brown, B.S., Wymore, R.S., Cohen, I.S., Dixon, J.E. & McKinnon, D. (1998) KCNQ2 and KCNQ3 potassium channel subunits: molecular correlates of the M-channel. *Science*, **282**, 1890-1893.

Waroux, O., Massotte, L., Alleva, L., Graulich, A., Scuvée-Moreau, J., Liégeois, J.-F. & Seutin, V. (2005) SK channels control the firing pattern of midbrain dopaminergic neurons in vivo in the rat. *Eur. J. Neurosci.*, **22**, 3111-3121.

Zweifel, L.S., Parker, J.G., Lobb, C.J., Bainwater, A., Wall, V.Z., Fadok, J.P., Darvas, M., Kim, M.J., Mizumori, S.J.Y., Paladini, C.A., Phillips, P.E.M. & Palmiter, R.D. (2009) Disruption of NMDAR-dependent burst firing by dopamine neurons provides selective assessment of phasic dopamine-dependent behavior. *Proc. Natl. Acad. Sci. USA*, **106**, 7281-7288.

Figure legends

Figure 1

XE991 selectively enhances burst firing of DA neurons *in vivo*, and increases the proportion of short interspike intervals in bursts. (a) M-current blockade was induced by a systemic administration of XE991 (3 mg/kg i.p.). A GABA_A antagonist (SR95531) was also iontophoresed (1mM, 100nA) during these recordings to block the most important inhibitory afferences. (b) Local M-channel blockade was performed by iontophoresis of XE991 (1 mM,

100 nA). Events which are underlined correspond to bursts (see Methods for our criteria). **(c)** Histogram showing a significant potentiation of bursting of DA neurons during M-current blockade (intraperitoneal XE991, $n = 6$; iontophoresed XE991, $n = 8$). **(d)** Both i.p. and local XE991 applications induced a significant shift of ISI's toward the shorter intervals, as also illustrated by the insets in **(a)** and **(b)**. (*, $p < 0.05$).

Figure 2

XE991 increases fast firing in dopaminergic neurons *in vitro*. **(a)** Intracellular recording showing that a given amount of current (+ 120 pA) elicits more spikes (truncated in the figure) in the presence of XE991. The experiment was performed in the presence of 300 nM apamin, 10 μ M CNQX, 50 μ M APV, 10 μ M SR95531 and 1 μ M CGP55845. Baseline membrane potential was set at -60 mV by a continuous injection of -100 pA. The speed of the recording was reduced 100 fold at the beginning of the superfusion of XE991. **(b)** Summary plot showing the time-course of the effect of XE991 ($n = 4$). (**, $p < 0.01$; ***, $p < 0.001$ versus control)

Figure 3

Simulations of M-current blockade on a DA neuron model confirm its selective effects on burst firing. **(a) Example of a simulation.** M-current inhibition was modeled by setting the M-current conductance to 0, while the effect of NML was modeled by reducing the $I_{K,SK}$ conductance (in this case to 0). The temporal pattern of synaptic inputs was exactly the same in the four traces **(b)** Simulations ($n = 6$) showed a significant potentiation of bursting of the model DA neuron during M-current inhibition. **(c)** A significant shift of ISI's toward the shorter intervals is seen in the model, as also illustrated by the insets in **(a)**. **(d)** Effect of $I_{K,SK}$

and combined $I_{K,SK}$ and $I_{K,M}$ inhibitions on the relationship between $[Ca^{2+}]_{in}$ and intra-burst firing rate. (**, $p < 0.01$; ***, $p < 0.001$).

Figure 4

Charge transfer through M channels in the model when SK channels are present or absent. (a) Values of the membrane potential (top) and the amplitude of the M-current (bottom) in control conditions (left) and during a $I_{K,SK}$ inhibition (right). **(b)** Overall M-current density in model. **(c)** M-current density 20 ms before action potentials in model ($n > 200$ events in 6 modeled cells). The overall M-current density during $I_{K,SK}$ inhibition is only twice that in control conditions. However, the amount of M-current that opposes the generation of action potentials is much larger during $I_{K,SK}$ inhibition. $p < 0.001$ between control and $I_{K,SK}$ inhibition (Student's t-test for paired values (b) and Student's t-test for unpaired values (c)).

Figure-1 (Seutin)

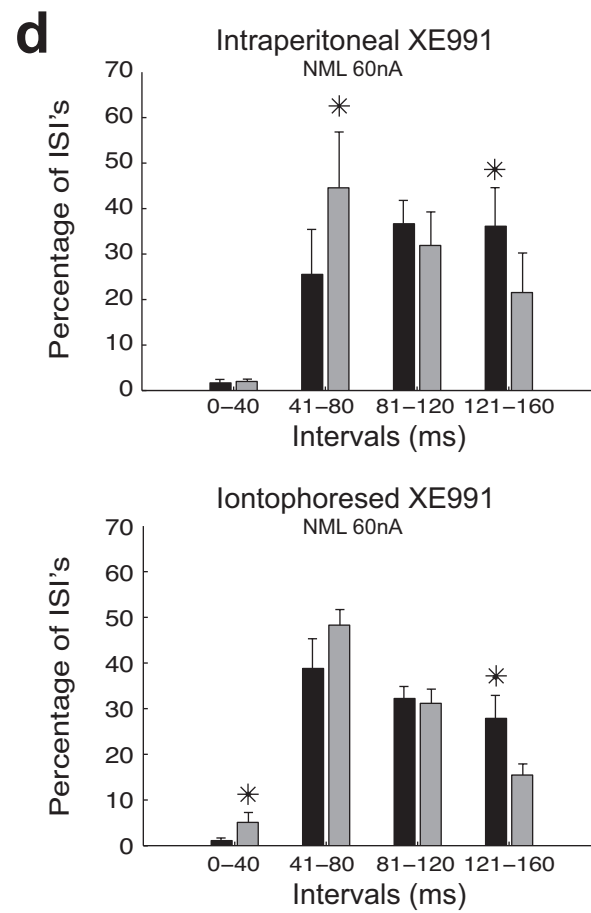
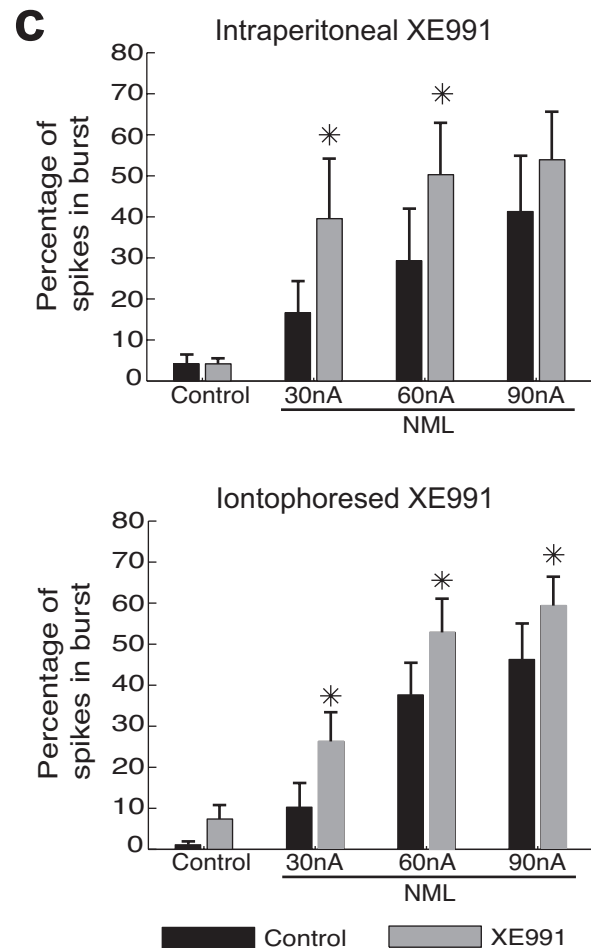
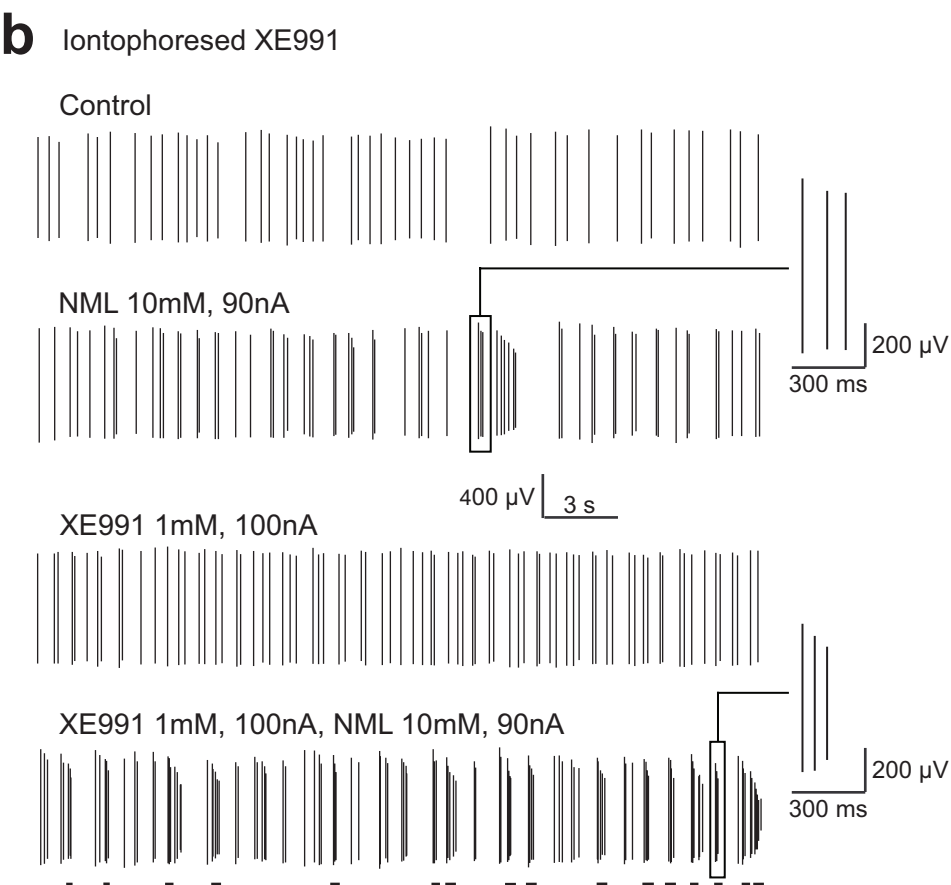
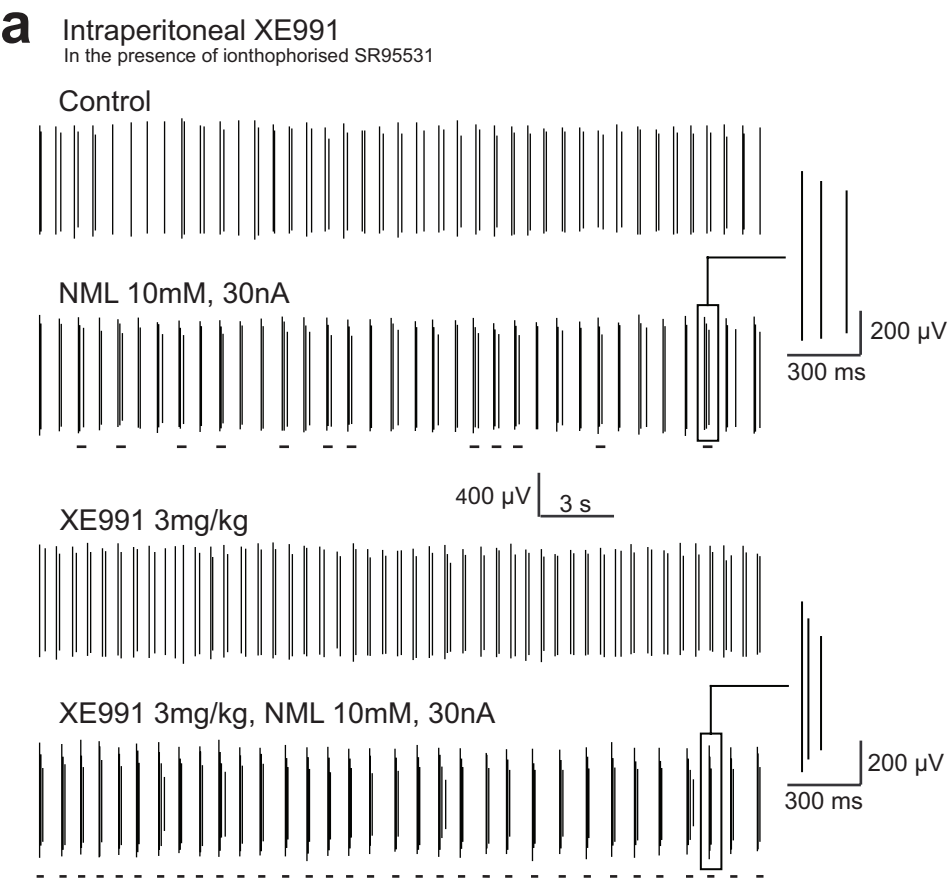


Figure-2 (Seutin)

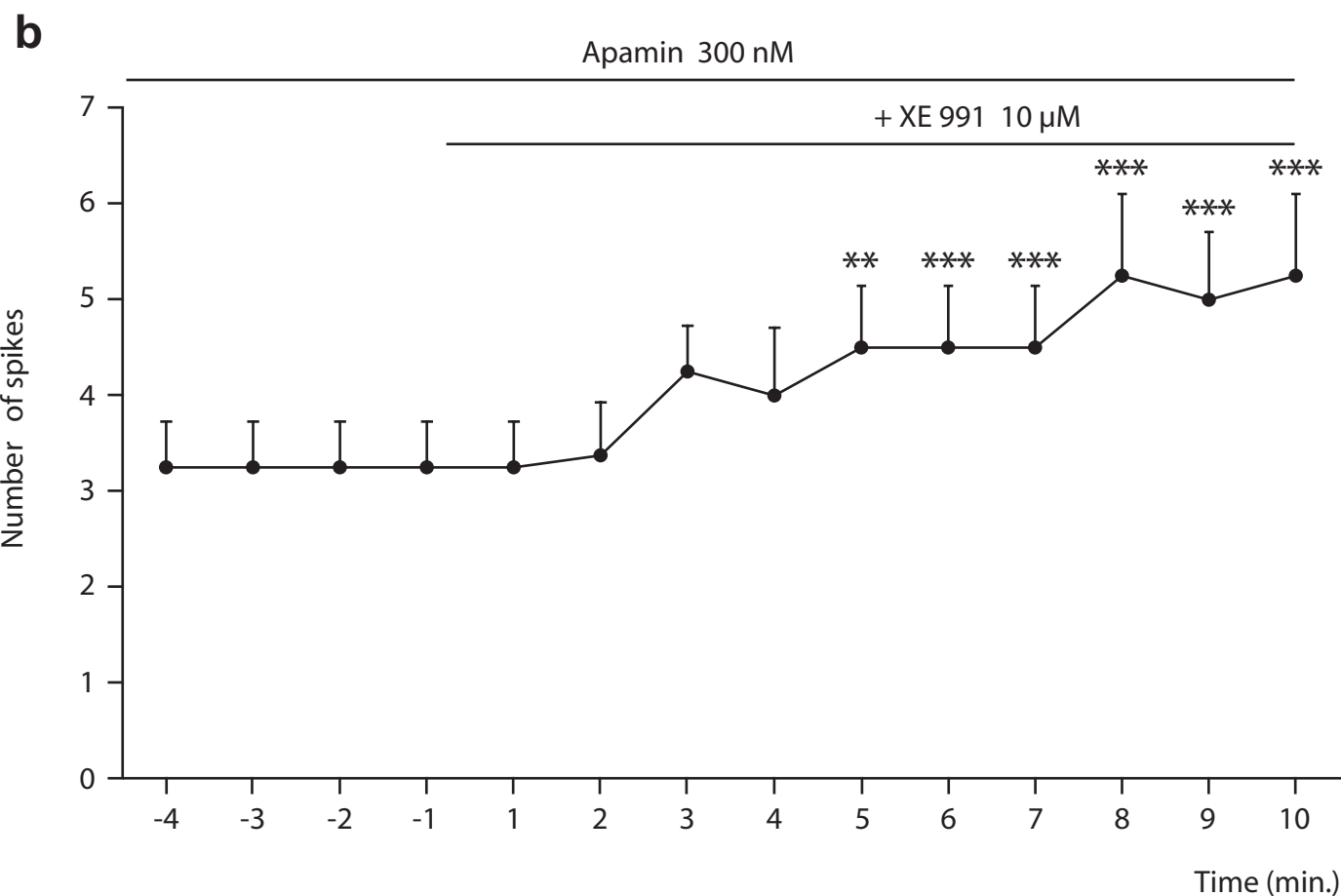
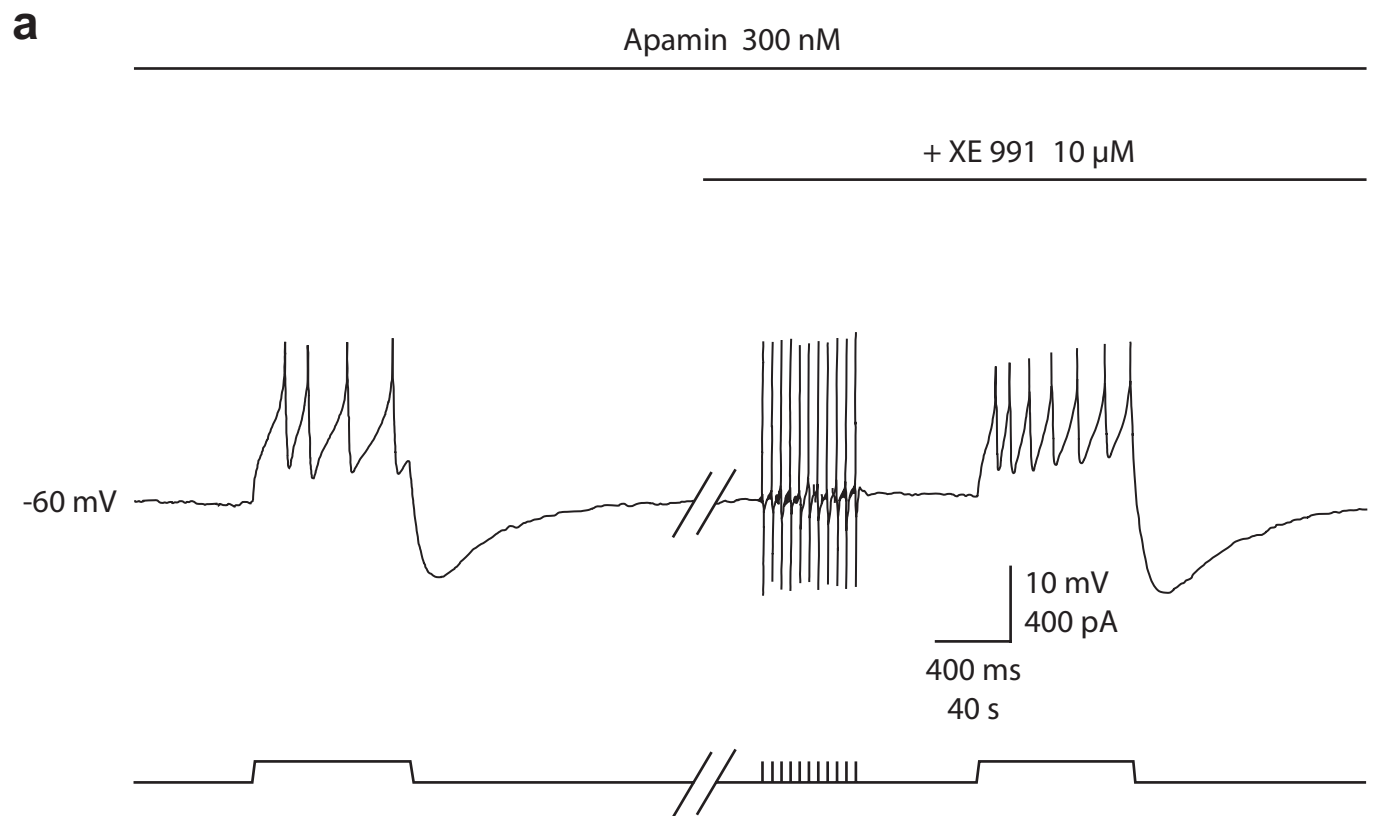
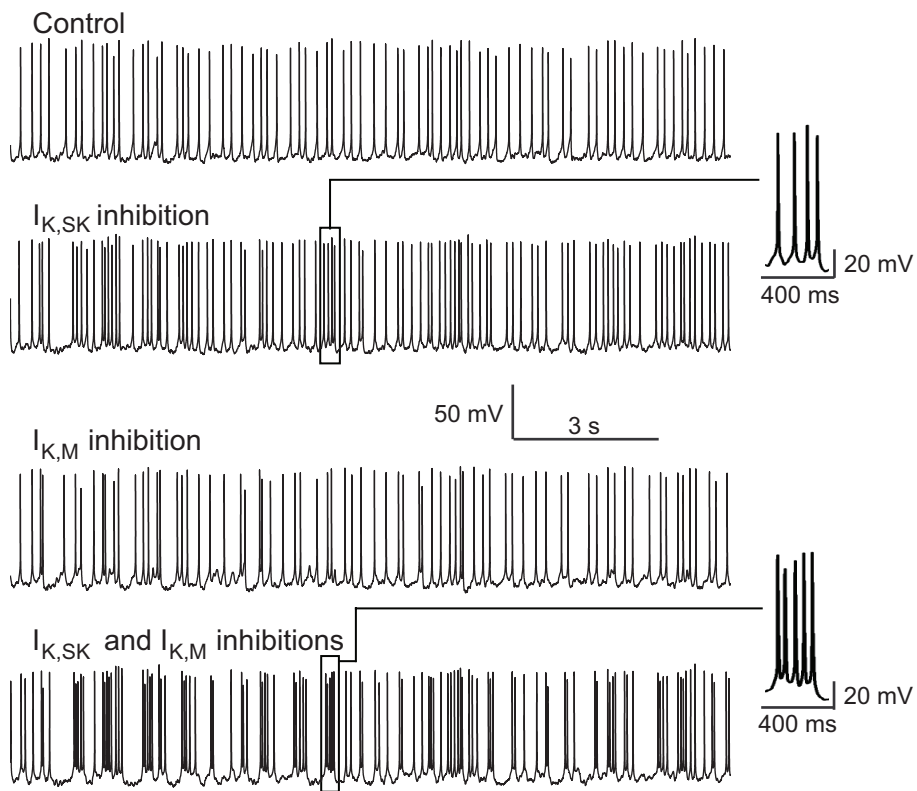
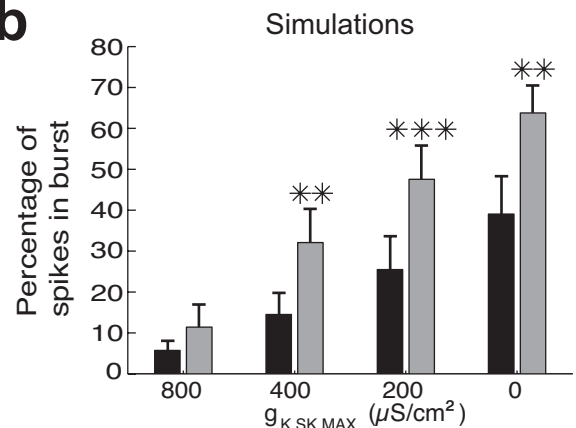
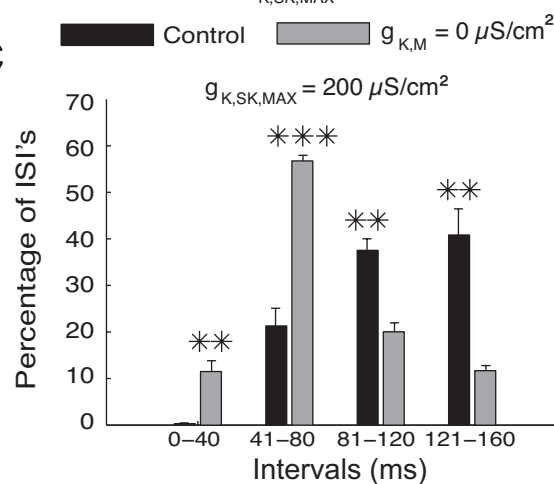


Figure-3 (Seutin)

a Simulations**b****c****d**

Intra-burst firing frequency as a function of the intracellular calcium concentration in the model

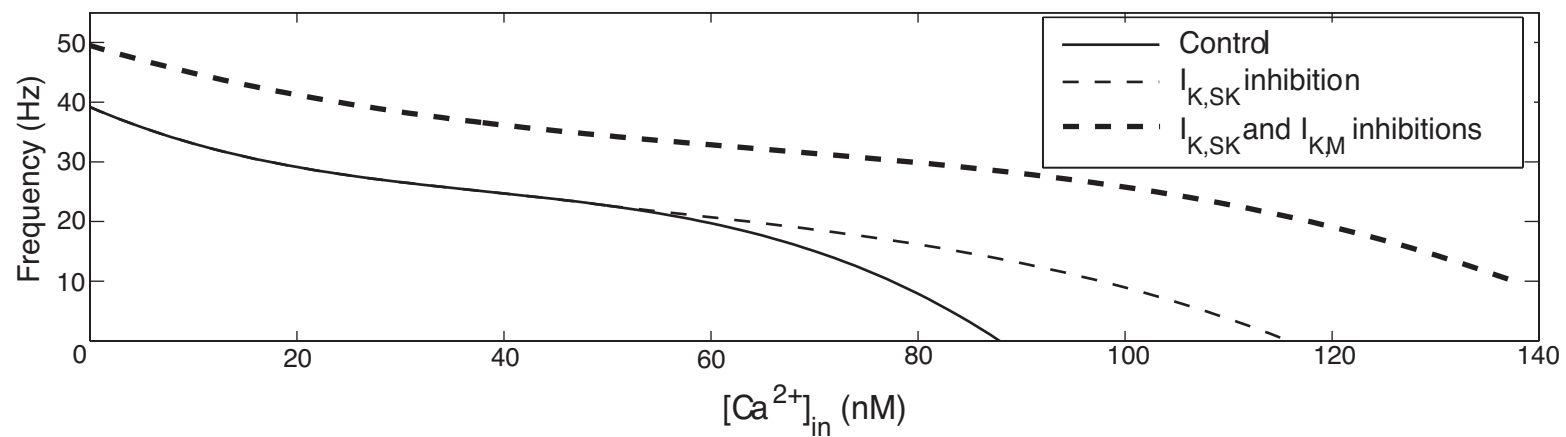


Figure-4 (Seutin)

